2D elastic finite element method (fem) for deformation analysis of the seismic and post-seismic cheliff (algeria) geodetic network

B.GOURINE
Centre des Techniques Spatiales (CTS), Division de Géodésie Spatiale, BP n°13, 1 av. de la Palestine, Arzew – Algérie
Email: bachirgourine@yahoo.com; bgourine@cts.asal.dz

Abstract: The region of Cheliff , located at the North West of Algeria, is of an exceptional interest for the study of crustal motion due to seismic activity. However, it is classical to represent the correspondent deformations according to displacement vectors and strain tensors. Through this present work, we propose a solution based on the finite element method (FEM) to refine the estimation and the representation of the geodetic networks deformation. In this context, a study of the deformation is carried out to analyze the horizontal motion of the Cheliff geodetic network due to the famous earthquake of October 10, 1980 (Ms = 7.3), based on two-dimensional elastic finite element model. The network was observed by classical triangulation in 1976 (by INCT) and 1981 (by CRAAG). The different results are illustrated in terms of displacement vectors, strain and stress tensors. Estimated deformation is interpreted according to previous geophysical studies which revealed a compressive phenomenon of Cheliff area, in the NNW-SSE orientation, due to the rapprochement of the African and Eurasian tectonic plates, and a block rotation phenomenon, at the SE and NW parts of the fault, in a retrograde direction. The study was extended to the post-seismic geodetic network observed between June1990 and April 1992. This network, established by distance measurements, is composed of 12 monitoring points distributed along the reverse fault. The results show a post seismic meaningful deformation, in the fault central segment, characterized by global NW-SE direction of strain tensors in agrees with ground data.

Key Words: Deformation, Finite element method, Strain Tensor, Stress tensor, Geodetic Network.

1. Introduction

Measuring the deformation of geodetic networks is an operation that, sometimes, takes a great economic or scientific importance. It is used in many cases, for example to monitor almost the big structures (dams, bridges, storage tanks, ...) (Gourine et al. 2012), but also to follow certain natural phenomena capable of inducing significant natural hazards such as landslides, earthquakes, crustal movements, etc. Such measurements are important to knowing the mechanical functioning of the lithosphere, under variable constraints.

Generally, the methodology employed consists in establishing a precise and homogeneous geodetic network, covering the area of study. The network benchmarks are determined thanks to terrestrial and/or space positioning techniques (GNSS). The reiteration of the observations of the same network, after a certain period, permits to detect the movements appeared during this time, by coordinate's variation estimation.

There are two methods to evaluate these movements (Welsch 1983; Prescott et al. 1979): vector-displacements and strain tensors. Considered as gradient of the displacement field, the strain tensors represent a very efficient tool to perform the deformation computation and can be very helpful to analyse the behaviour of the studied area (Pagarette et al. 1990). Unlike to the vector-displacements, they are independent of any reference frame which makes very delicate the interpretation of the movements. Nevertheless, the strain tensors computation depends on the configuration of the selected elementary figures formed from the geodetic points. This constraint makes difficult the interpretation of the results obtained (Gourine and Ghezali. 2013).

To overcome this drawback, the finite element method (FEM) presents an appropriate solution for homogeneous and continuous representation of network deformation (Abolghasem and Grafarend 2003; Gourine and Ghezali 2013). This method has become one of the most important and useful engineering tools for engineers and scientists. It is a numerical procedure, generally used for solving engineering problems (represented by partial differential equations with boundary conditions) with considering the physical and mechanical properties of the

The objective of this paper is double. In one hand, it consists of the application of the FEM to evaluate the deformations of the geodetic network of Cheliff (North of Algeria) due the famous earthquake of October 10, 1980 (Ms = 7.3), and in other hand, to study the post seismic activity of this region.

The data concern the seismic geodetic network of Cheliff observed by classical triangulation in 1976 and 1981, and post-seismic geodetic network measured by distance measurements in 1990 and 1992, see section (2).

The analysis methodology adopted, based on FEM, is described in section (1). The different results obtained are presented and discussed in section (3).

2. Finite Element Method

The finite element method is a numerical procedure for solving engineering problems which are represented by partial differential equations (PDEs), with boundary conditions. It assumes discretization of the domain by a set of subdomains called the finite elements.Throughout this paper, linear elastic behaviour is assumed.

According to the fundamental equations of continuum mechanics, the equations of motion and compatibility equations of displacements of a volume V of limit S can be derived. Therefore, the general equations of the boundary value problem in solid mechanics are expressed as follows:

$$\begin{cases} \varepsilon = L \cdot U \\ L^T \sigma + P = 0 \\ L_1^T \sigma = q \\ \sigma = f(\varepsilon) \end{cases} \quad \textbf{(1)}$$

where ε denotes the strain deformation vector and σ is the stress vector, P is the vector of force volume, q is the vector of force surface, U is the displacement vector, L and L_1 are differential operators. A linear elastic medium may be modelled directly by using the displacement of finite elements method. The equilibrium condition of displacement for approximation by finite element is given by (Richardson 1978):

$$[K] \cdot \{U\} = \{F\} \quad (2)$$

where:

$[K]$ is the global stiffness matrix.

$\{U\}$ is the vector of displacements of the nodes for the whole structure, in a global coordinate system.

[F] is the vector of loads on the structure.

Generally, the external loads are known and the stiffness matrix can be formed once the geometry and the elastic properties of the structure are specified. Equation (1) is usually regular and with full rank, so the unknown nodal displacements can be solved.

If the coordinates of geodetic network points are known, the displacements calculated from these data provide the boundary conditions of the nodal displacements with the corresponding equation:

$$U\big|_S = U_0 \quad (3)$$

The fields of displacement, strain tensor and stress tensor can be determined from equations (2) and (3) using the finite element method (FEM). In our case, to assess the horizontal deformation of geodetic network, the problem of plane elasticity can be defined as follows:

$$\{U\} = \begin{bmatrix} u \\ v \end{bmatrix}, \quad \{\sigma\} = \begin{bmatrix} \sigma_x \\ \sigma_y \\ \tau_{xy} \end{bmatrix}, \quad \{\varepsilon\} = \begin{bmatrix} \varepsilon_x \\ \varepsilon_y \\ \gamma_{xy} \end{bmatrix} \quad (4)$$

where u and v are the displacement components in the x and y directions. The strains vector $\{\varepsilon\}$ is:

$$\{\varepsilon\} = \begin{bmatrix} \dfrac{\partial u}{\partial x} \\ \dfrac{\partial v}{\partial y} \\ \dfrac{\partial u}{\partial y} + \dfrac{\partial v}{\partial x} \end{bmatrix} = [B] \,.\, \{U\} \quad (5)$$

where $[B]$ is a differential operator, as:

$$[B] = [\, B_1 \;\; B_2 \;\; .. \; B_i \;\; .. \;\; B_n]_{2xn}$$

with n is number of nodes

$$[B_i] = \begin{bmatrix} \dfrac{\partial N_i}{\partial x} & 0 \\ 0 & \dfrac{\partial N_i}{\partial y} \\ \dfrac{\partial N_i}{\partial y} & \dfrac{\partial N_i}{\partial x} \end{bmatrix}$$

with N_i is the interpolation function which can be expressed by:

$$N(\xi,\eta) = \begin{bmatrix} \frac{1}{4} \cdot (1-\xi) \cdot (1-\eta) \\ \frac{1}{4} \cdot (1+\xi) \cdot (1-\eta) \\ \frac{1}{4} \cdot (1+\xi) \cdot (1+\eta) \\ \frac{1}{4} \cdot (1-\xi) \cdot (1+\eta) \end{bmatrix}$$

The partial derivates of this function are (Dhatt and Touzot 1981):

$$\frac{\partial N}{\partial \xi} = \begin{bmatrix} \frac{1}{4} \cdot (-1+\eta) \\ \frac{1}{4} \cdot (1-\eta) \\ \frac{1}{4} \cdot (1+\eta) \\ \frac{1}{4} \cdot (-1-\eta) \end{bmatrix} \text{ and } \frac{\partial N}{\partial \eta} = \begin{bmatrix} \frac{1}{4} \cdot (-1+\xi) \\ \frac{1}{4} \cdot (-1-\xi) \\ \frac{1}{4} \cdot (1+\xi) \\ \frac{1}{4} \cdot (1-\xi) \end{bmatrix}$$

ξ, η: are the nodal local coordinates of an element.

For an isotropic material, the relationship between strains and stresses obeys to Hooke's law and can be expressed by:

$$\{\sigma\} = [D] \,.\, \{\varepsilon\} \quad (6)$$

[*D*] is the property material matrix, such as:

$$[D]=\frac{E}{1-\nu^2}\begin{bmatrix}1 & \nu & 0\\ \nu & 1 & 0\\ 0 & 0 & \frac{1-\nu}{2}\end{bmatrix}$$

Where E and are, respectively, Young modulus (N/m²) and Poisson's ratio (unitless).

Generally, we can summarize the finite element analysis method as follows, (Oudin 2008):

- Step 1. Discretizing the domain – this step involves subdividing the domain into elements and nodes. For continuous systems like plates and shells this step is very important and the answers obtained are only approximate. In this case, the accuracy of the solution depends on the discretization used.

- Step 2. Computation of the element stiffness matrices – the element stiffness equations need to be computed for each element in the domain.

- Step 3. Assembling the global stiffness matrix.

- Step 4. Applying the boundary conditions – like supports and applied loads and displacements.

- Step 5. Solving the equations – this will be done by partitioning the global stiffness matrix and then solving the resulting equations using Gaussian elimination.

- Step 6. Post-processing – to obtain results as the reactions and element forces, strains and stresses.

The following figure illustrate the flow-chart of the FEM method adopted for the Cheliff network.

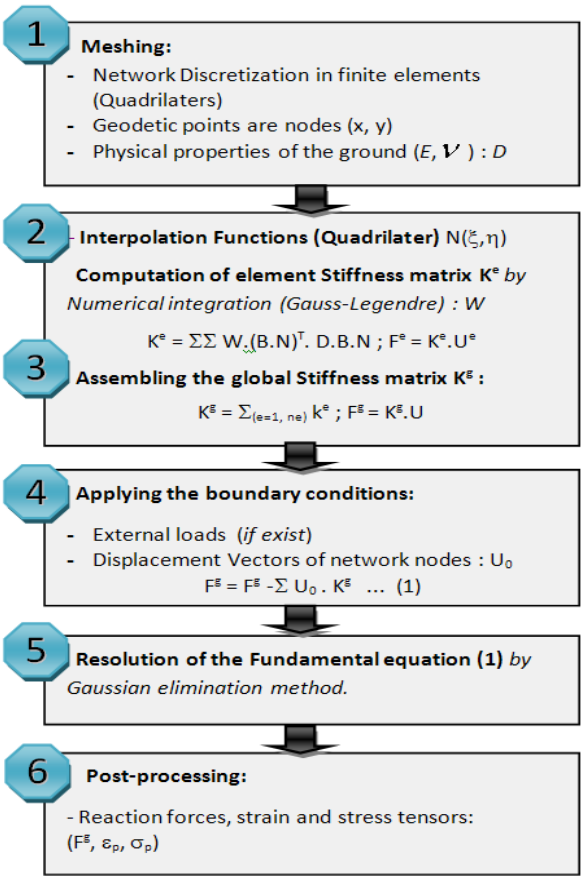

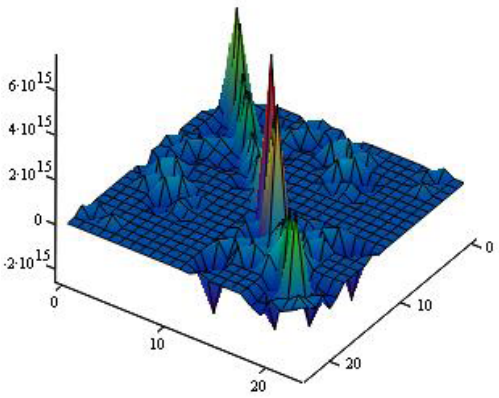

Structure of global Stiffness (*case of post-seismic network*)

Fig. 1 Flow-chart of the FEM applied to Cheliff network (Gourine et al., 2013).

3. Study Area

3.1 Seismic Context of the region

The region of Cheliff (ex-El Asnam)is the most active area in Algeria that marks the confrontation of African and Eurasian tectonic plates where there have been several earthquakes of Magnitude > 5, (Mc Kenzie 1972). It is characterized by the plain of Lower Cheliff. In the coarse East-West (EW) direction, this region is limited in the north by Dahra's mountain, which is extended to the Mediterranean Sea and in the south by the mountains of the Ouarsenis. The Basin formation of Lower Cheliff enters in the framework of recent tectonics affecting the western Mediterranean region. Indeed, old and recent studies have shown that the Europe-Africa tectonics collision, more active in the North African chain, induced to a compressive tectonic in the NNW-SSE direction where are associated reverse faults (Philip and Meghraoui 1983). On the other hand, this movement of Continent-Continent collision is described as the result of the rotation of Africa around an axis (rotation pole in Rabat, Morocco) (Mc Kenzie 1972) and (Minster 1978).

This intense neotectonic region is marked on the surface by seismic fault of Oued Fodda (Cheliff). This fault is caused by the famous earthquake of October 10, 1980 in the NE-SW, which left the North West block overlaps the South East block over 40 km length.

3.2 Monitoring geodetic networks

The Centre for Research in Astronomy, Astrophysics and Geophysics (CRAAG) has conducted geodetic observations to study the crustal movements related to the seismicity of the region of Cheliff and particularly the study of the fault caused by the earthquake of October 10, 1980. In June 1981, the first assessment of vertical and horizontal movements by geodetic methods was carried out by re-observing the local geodetic network which was already established by the National Institute of Cartography and Remote Sensing (INCT) in 1976.

The observed triangulation network is constituted of 14 geodetic points distributed on both sides of the fault. Geographically, it is limited between (1 ° 19 'and 1 ° 39' East) in longitude and (36 ° 02 'and 36 ° 23' North) in latitude (Merbah et al. 2005), figure (2). The number of points are designed by alphabetical letters (A, B, .., N). In 1976, the network had been observed only with angular measurements using first-order triangulation procedures and WILD T3 Theodolites. The accuracy was estimated at a few decimetres for relative position of the different points. A second observation campaign was conducted in 1981, using the same procedures and instruments. The Geodimeter AGA 14A was used to measure distances in the northern and southern parts, in order to provide a precise scaling of the network (Ruegg et al. 1982).

To assess the post-seismic effect on the region, another monitoring network was established inside the Cheliff geodetic network. Limited between (1°24' and 1°36' East) in longitude and (36°07' and 36°15' North) in latitude, this network was carried out to supervise the reverse fault and to assess the evolution of ground deformation surrounding this fault (Ruegg et al. 1982).The network considered consists of 12 points including 03 reference points and 09 monitoring points. It was observed by trilateration during two observation campaigns, in June 1990 and April 1992 (works undertaken by the CRAAG). The number of points are designed by Arabic numbers (101, 102, .., 112). The majority of measured triangle sides vary between 4.5 km and 7.3 km and the modal value is 6 km. The distances between network points were measured with the distance meter (Di20) with accuracy of about ±5mm+10-6D (km). They are corrected from atmospheric effects and reduced according to the UTM projection associated to Clarke 1880A reference ellipsoid of Nord Sahara 1959 (NS-59) datum. The estimated accuracy of the network point is about of few centimetres.

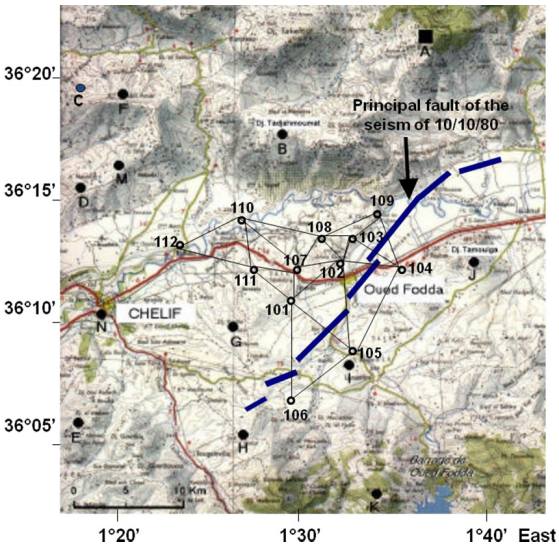

Fig. 2 Map of both Cheliff monitoring geodetic networks according to 1976-1981 and 1990-1992 periods.

4. Results and discussion

The Least Squares compensation of the observations of both monitoring networks leads to assess the final coordinates of the points and their precisions. The absolute error ellipses are computed from the estimated parameters variance covariance matrix. The figure (3) depicts the 1-σ error ellipses between 1990 and 1992 period.

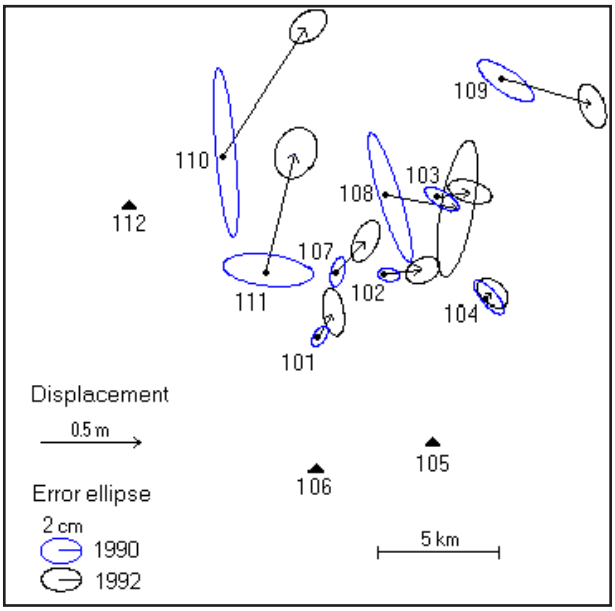

Fig. 3 Comparison between 1990 and 1992 campaigns.

In our case, the adopted values of the physical characteristics of the region are given by:

$$\begin{bmatrix} E \\ \nu \\ b \end{bmatrix} = \begin{bmatrix} 100 \times 10^9 \\ 0.3 \\ 15000 \end{bmatrix}$$

These values displayed are simulated. However, they are taken from similar case of geodetic monitoring networks as that of the Cheliff region (Dingbo et al. 1996). The ground thickness b (m) is taken from (Ruegg et al. 1982).

Figure (4) illustrates the deformation results related to the seismic monitoring network. The displacement vectors of the points (H, I, J) and (M, B, L) are directed in two opposite directions, NW and SE, respectively, according to the fault. The displacement vectors of the other points (K, G, E, D, F, C) describe a block rotation in retrograde direction. In another hand, a shortening phenomenon of distances is observed between network nodes, particularly those located on both sides of the main fault, which can reach -2 m, this justifies the hypothesis of compressive motion and overlapping NO part over the SE one, given by geophysicists.

For the strain tensors, which are depicted according to the deformation principal components, the results show a predominance compression of about -150 ppm, especially on both sides of the main fault with maximum of -360 ppm, with perpendicular directions. This global trend of NW-SE shortening is similar to that deduced by tectonic observations (Philip and Meghraoui 1983) or focal mechanisms (Cisternas et al. 1982). The presence of distensive faults on overlapping compartment, area where the movements are generally compressive, is due to an extrados extension and to gravitational effects (Philip and Meghraoui 1983). There is also a change in direction of the deformation tensors from NW-SE to NE-SW, in the retrograde direction, from SW to NW of the fault, which confirms the presence of a block rotation phenomenon.

According to (Ruegg et al. 1982), we are in a case of inelastic finite dislocations (presence of fault and fracture). Therefore, the mean deformation tensor is only a compact and intrinsic representation of the deformation within the finite element considered. However, it would be wise to consider the dislocation modeling of Cheliff network, by FEM. For this purpose, recent studies about dislocation based FEM modeling have been conducted by (Abolghasem and Grafarend 2003) and (Güney et al. 2010).

The dilatation is represented by circles with proportional radii to deformation amplitudes. The red circles are dilatations and the blue ones are compressions. These later are observed over the entire of study area, particularly along the fault. Large compressions, of about -180 ppm, are on the SW extremity of the fault which indicate the block rotation and overlapping of NW block on East one. However, some points have undergone dilatations of about 30 ppm, such as (B, C, E and I). The shear expresses the change of configuration of the element. The results indicate high deformation of about 250 ppm around the fault, except for the NW region where the shear is weak and at level of 20 ppm.

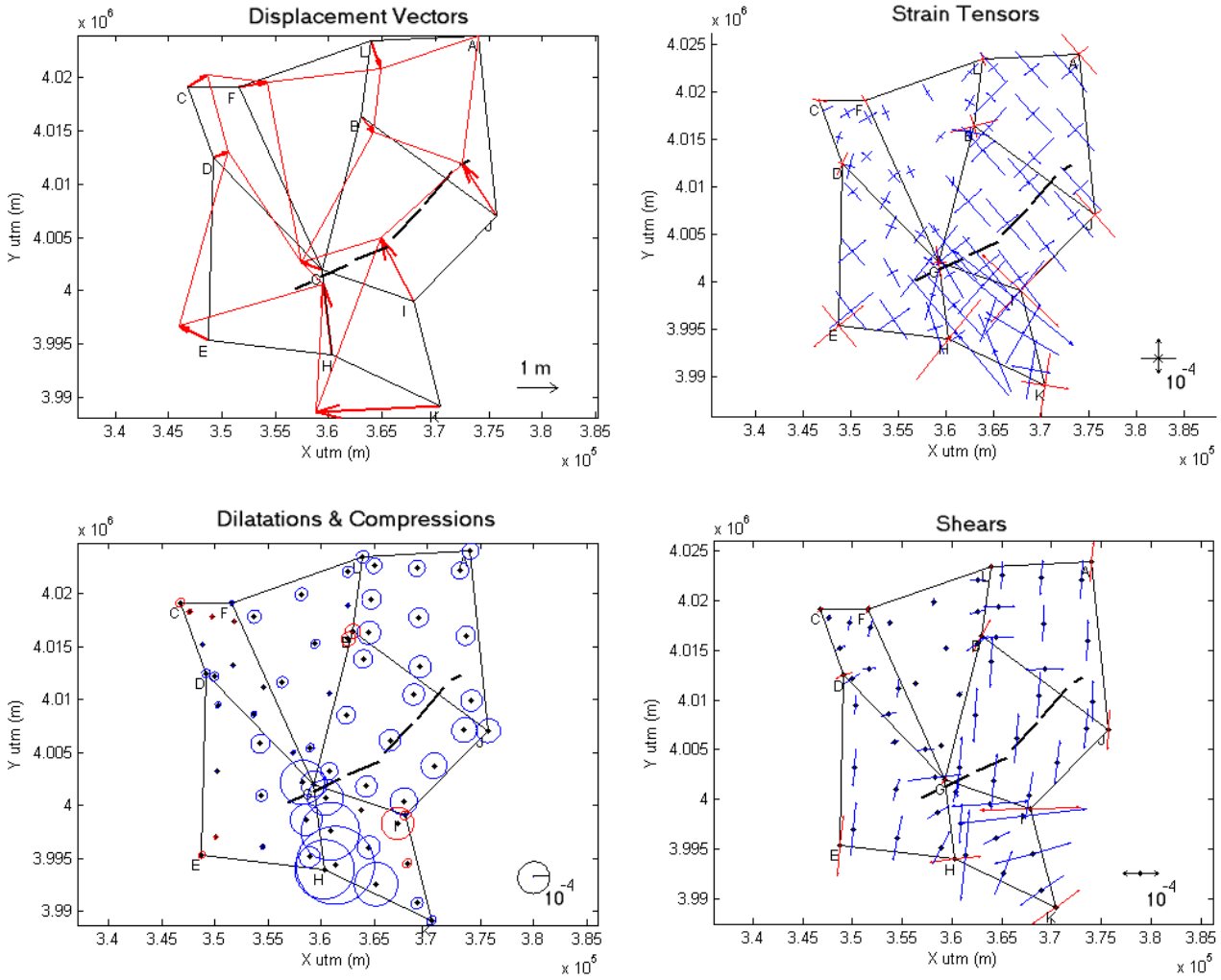

Fig. 4 Displacement vectors and deformation field by 2D FEM of the Cheliff seismic geodetic network.

Figure (5) illustrates the deformation results related to the post-seismic monitoring network. The average of displacements vectors are of about 30 cm. The maximum value is reached at the point 110 with 68 cm. The orientation of these vectors describes a rotation in NE-E direction. One can distinguish two regions of deformation. The first concerns the compression which is surrounding the fault of range of 10-100 ppm with maximum of 400 ppm at the point 107. However, the second one concerns the dilatation, mainly is in the North part of about 10-60 ppm. Total shears of these regions are represented by vectors proportional to their values which are enough intense, particularly at the north side of the fault with NW-SE direction.

Such results confirm the hypothesis proposed by (Ouyed et al. 1983) which consists of the existence of two sliding dextral faults in the NW-SE direction, explaining the shift between the central segment and SE segment of the fault.

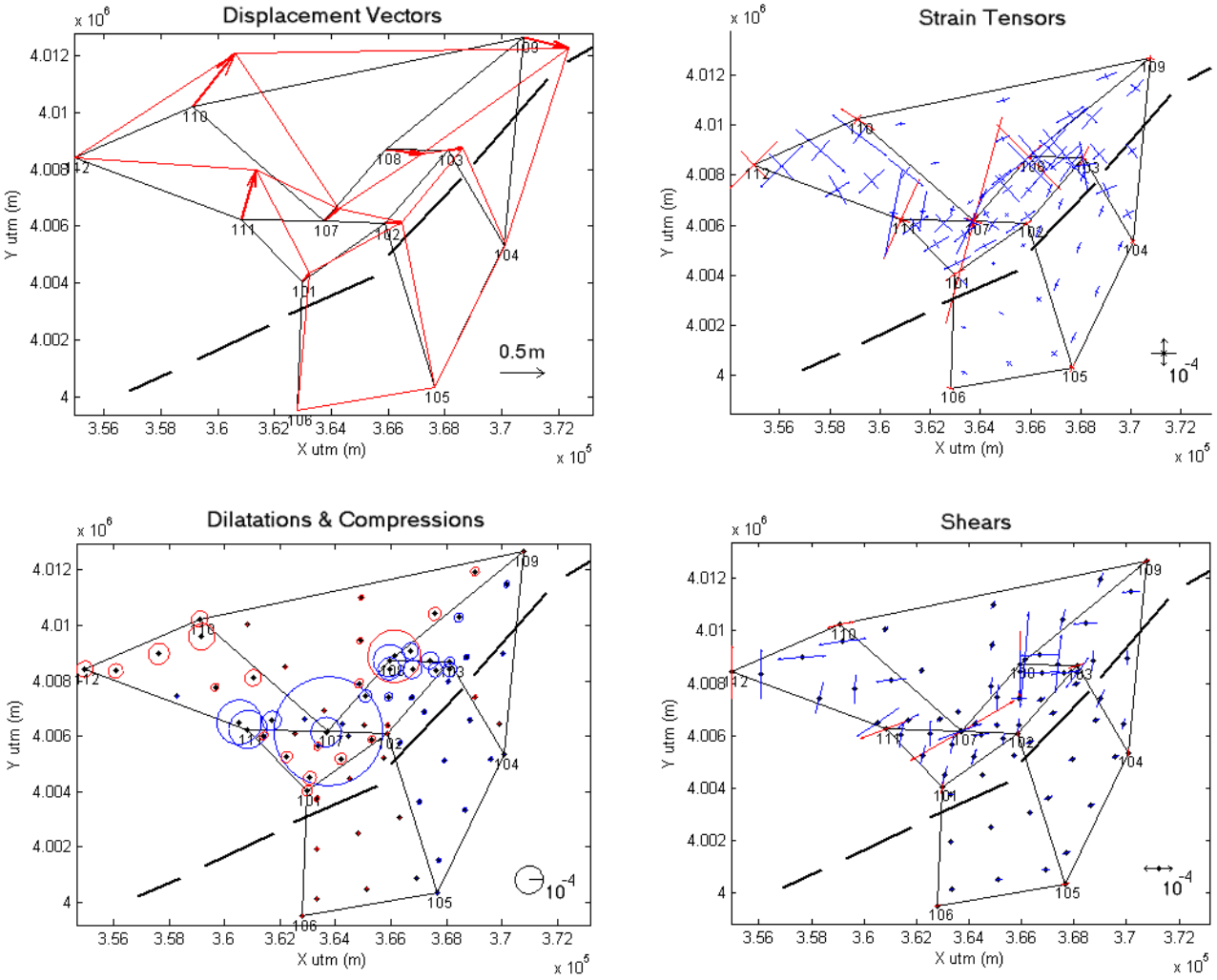

Fig. 5 Displacement vectors and deformation field by 2D FEM of the Cheliff post-seismic geodetic network.

Figure (6) shows the applied reaction forces on both networks. It should be noted that the determination of the reaction forces at nodes of the network depends mainly on the physical characteristics of the area. These parameters are simulated in our case. The seismic period is characterized by significant forces on both sides of the main fault in two opposite directions NW and SE. Important magnitudes are observed in the SE part of the area where the maximum force is at point I. The majority of force vectors are directed in opposite directions (NNW-SSE) indicating a significant compressive phenomenon. The post-seismic period is characterized by the same behaviour but with lower magnitudes.

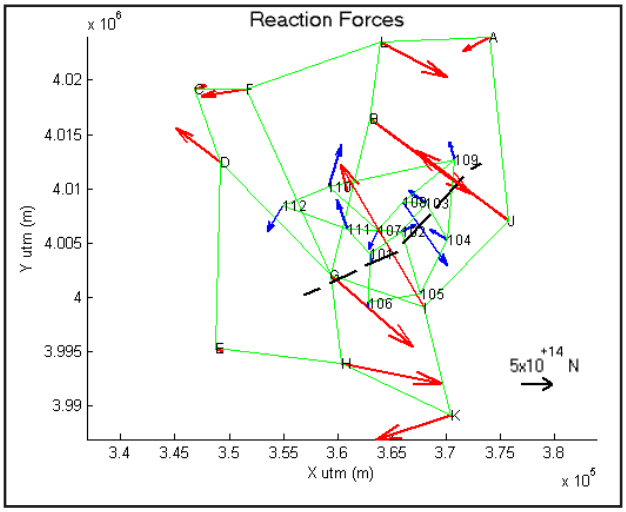

Fig. 6 Reaction forces vectors of both monitoring networks. Red and blue vectors correspond to seismic and post-seismic networks, respectively.

Figure (7) depicts the principal stress tensors according to both networks. In figure (7.a), the zones near the fault have undergone significative stresses with 40 MPa (at SW side of fault). Figure (7.b) shows significative stresses of around of 20 MPa at North and NW parts of fault, indicating a presence of post-seismic activity, in the region. 4.

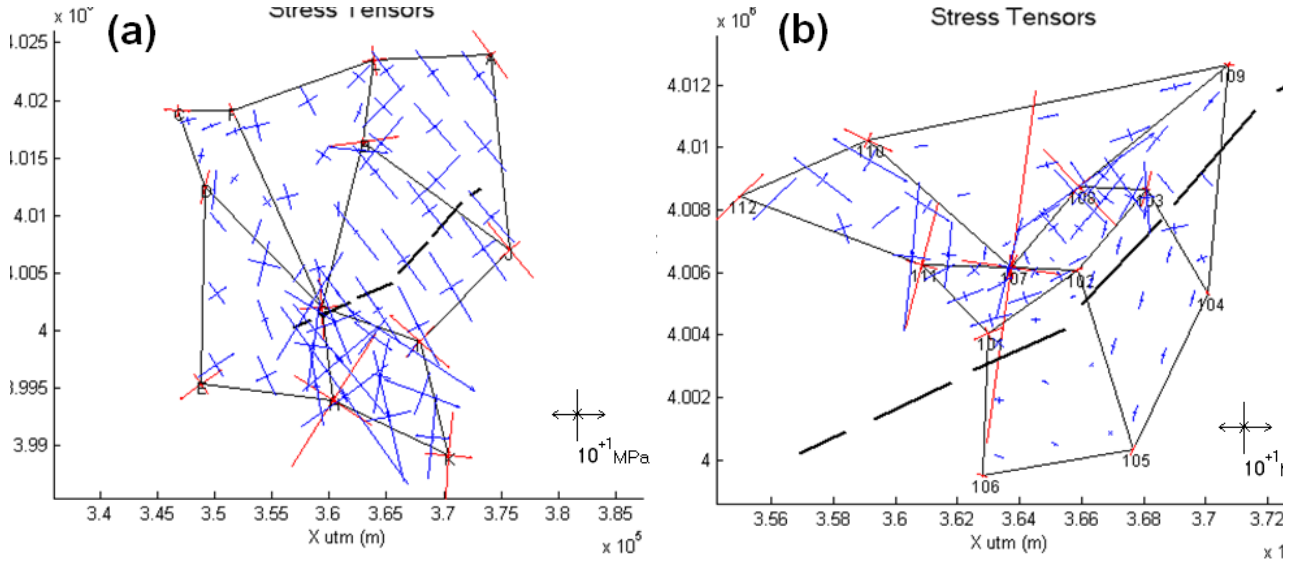

Fig. 7 Principal stress tensors of both networks by 2D FEM. (a) seismic geodetic network, (b) post-seismic geodetic network.

5. Conclusion

Through this paper, the finite element method (FEM) was successfully applied in the estimation and representation of deformations of Cheliff monitoring networks which allows easy reading of horizontal movements. Our results show, in one hand, the performance of the adopted FEM in the modeling and analysis of strain and stress tensors, and in other hand, they have highlighted geophysical phenomena as following:

- A compressive phenomenon, in the NNW-SSE direction, due to the rapprochement of the African and Eurasian tectonic plates that caused the thrust fault of the famous earthquake of 10 October 1980.
- A block rotation phenomenon, at the SE and NW parts of the fault, in a retrograde direction.
- A significant post-seismic deformation at level of the central segment of the fault which can be considered as a pre-seismic factor to not neglect.

For FEM developing in the deformation domain, the following points should be investigated:

- Performing statistical analysis of deformation errors by Monte Carlo method (Michel et al. 2003);
- Application of 3D FEM to evaluate deformations of 3D geodetic networks (GPS);
- Adoption of dislocation model with FEM deformation representation.

Références bibliographiques

Abolghasem M, Grafarend EW (2003) Finite element analysis of quasi-static earthquake displacement fields observed by GPS. J. of Geod.,Vol. 77, No. 9, 529-536.

Dhatt G, Touzot G (1981) Une présentation de la méthode des éléments finis. Presses de l'Université Laval Québec, Maloine S.A. Ed. Paris, 543p.

Cisternas A, Dorel J, Gaulon R (1982) Models of the complex source of the EL-ASNAM earthquake. Bull. Seism. Soc. Am., Vol. 72, N°6, pp. 2245-2266.

Dingbo C, Caijun X, Jingnan L (1997) Analyses of the crustal deformations in the Tibetan Plateau with three dimension elastic finite element method. Sciences Reports 1996 of the school of Geoscience and Surveying Engineering, WTUSM (China), Ed. 1997, pp 01-09.

Güney D, Acar M, Özlüdemir MT, Celik RN (2010) Investigation of post-earthquake displacements in viaducts using Geodetic and Finite Element Methods. Nat. Hazards Earth Syst. Sci., 10, 2579-2587.

Gourine B, Mahi H, Khoudiri A, Laksari Y (2012) The GRNN and the RBF neural networks for 2D displacement field modelling. Case study: GPS auscultation network of LNG reservoir (Gl4/Z industrial complex – Arzew, Algeria). Proc. FIG Working Week 2012, Rome, Italy.

Gourine B, Ghezali B (2013) Analyse préliminaire des déformations du réseau géodésique de Cheliff (Algérie), entre 1976 et 1981, par la méthode des éléments finis 2D. Revue "Nature & Technologie", A-Sciences fondamentales et Engineering, n°08/Janvier 2013, pp 50-58, Issn: 1112-9778.

Mc Kenzie DP (1972) Active tectonics of the Mediterranean region. Geophys. J. R. Astron. Soc., 30: 109-185.

Merbah A, Gourine B, Ghezali B, Kahlouche S, Meghraoui M, Sevilla MJ (2005) Evaluation et interprétation des déformations horizontales et de leurs erreurs sur un réseau de surveillance sismique. Proc. FIG Working Week 2005 and GSDI-8 Cairo, Egypt.

Michel V, Person T (2003) From geodetic monitoring to de formation tensors and their reliability, Proc. 11th FIG Symp. on Deformation Measurements, Santorini, Greece.

Minster JB (1978) Present day plate motion. Geophys. Res. Vol. 83, N° B11, pp. 5331-5354, 1978.

Oudin H (2008) Méthode des éléments finis, Notes de Cours v.1, Ecole Centrale de Nantes - France.

Ouyed M, Yielding G, Hatzfeld D, King GCP (1983) An aftershock study of the El Asnam (Algeria) earthquake of 1980 October 10. Geophysical Journal of the Royal Astronomical Society, vol.73, issue 3 (pp. 587-768).

Pagarette J, Kasser M, Ruegg JC (1990) Évaluation et représentation des erreurs sur les déformations d'un réseau géodésique : utilisation de la méthode de Monté Carlo. Bull. Géod. 64, pp 63-72.

Philip H, Meghraoui M (1983) Structural analysis and interpretation of the surface deformations of the EL-ASNAM earthquake of 10 October 1980. Tectonics, Vol. 2, N°1, pp. 17-49.

Richardson RM (1978) Finite element method of stress in the Nazca plate: driving forces and plate boundary earthquake. Tectono-physics, 50, pp 223-248.

Prescott WH, Savage JC, Kinoshita WT (1979) Strain accumulation rates in the western United States between 1970 and 1978. J. Geophys. Res., 84, 5423-5435.

Ruegg JC, Kasser M., Tarantola A, Lepine JC, and Chouikrat B (1982) Deformation associated with the EL-ASNAM earthquake of 10 October 1980: Geodetic determination of vertical and horizontal movements. Bull. of seismological society of America, vol. 72, n°6, pp 2227-2244.

Welsch W (1983) Finite element analysis of strain patterns from geodetic observations across a plate margin. Tectonophysics. 97, pp. 57-71.